Assessment of an inverse organic Rankine cycle system for the ECS of a large rotorcraft adopting a high-speed centrifugal compressor and a low GWP refrigerant

Ascione, Federica; De Servi, Carlo Maria; Meijer, Onno; Pommé, Vincent; Colonna, Piero

Publication date
2021

Document Version
Final published version

Published in
Proceedings of the 6th International Seminar on ORC Power Systems, 2021

ASSESSMENT OF AN INVERSE ORGANIC RANKINE CYCLE SYSTEM FOR THE ECS OF A LARGE ROTORCRAFT ADOPTING A HIGH-SPEED CENTRIFUGAL COMPRESSOR AND A LOW GWP REFRIGERANT

Federica Ascione[1]*, Carlo Maria De Servi[1], Onno Meijer[2],Vincent Pommé[3], Piero Colonna[1]

[1] Delft University of Technology, Propulsion and Power, Aerospace Engineering, Delft, The Netherlands

[2]Aeronamic B.V., Almelo, The Netherlands

[3]Airbus Helicopters, ECS & Thermal Departments, Marignane, France

*Corresponding Author: f.ascione@tudelft.nl

ABSTRACT

This study concerns the assessment of a novel concept for the Environmental Control System (ECS) of large rotorcraft, based on Vapour Compression Cycle (VCC) technology. Its uniqueness stands in the adoption of an electrically driven high-speed $6 - 8$ kW centrifugal compressor, in place of the traditional volumetric machine. A steady-state model of the system has been developed and implemented using the Modelica acausal modelling language. The working fluids selected for this investigation belong to the class of low-Global Warming Potential (GWP) refrigerants. The results show that to obtain feasible compressor designs, and in particular sufficiently large flow passages, a high molecular complexity fluid must be employed as it results in adequate volume flow rate. However, compared to fluids made of simpler molecules, heat exchangers are larger and possibly heavier. The tradeoff between thermodynamic performance, weight, volume, aircraft drag penalty and system integration in general is being investigated.

1 INTRODUCTION

The aerospace industry is, nowadays, urged to take measures to increase the sustainability of air transport, given the pace of the air traffic growth observed in the last decades and expected in the upcoming years. The consequent need to optimize aircraft and rotorcraft performance is calling for a step-change in the design practice of these systems, including their non-propulsive components. In this regard, it is envisaged that future aircraft and rotorcraft will feature only all-electric non-propulsive components to enable significant improvements in terms of aircraft weight, fuel consumption, total life cycle costs, controllability and maintainability. This change in the design paradigm of non-propulsive equipment is based on the More Electric Aircraft (MEA) or Rotorcraft (MER) general concept (Sarlioglu and Morris, 2015).

The auxiliary system guarantying cabin pressurization and thermal comfort, hereinafter indicated as Environmental Control System (ECS), is currently the primary consumer of non-propulsive power at cruise (AC-9B, 1989). The idea underpinning this study is that the efficiency and environmental footprint of ECS aboard aircraft or rotorcraft can be significantly improved by adopting a VCC for cabin cooling. This system features a high-speed centrifugal compressor driven by an electric motor as the prime mover and a low-GWP refrigerant as working fluid. The case study is a high payload helicopter. A steady-state system model was developed using the acausal modelling language Modelica to assess the thermodynamic performance as a function of several working fluids and verify the feasibility of the compressor and evaluate the size of the evaporator. Different low-GWP refrigerants were considered, such as hydro-fluoro olefins (HFOs) and hydrocarbons. The system model simulations are carried out for each refrigerant, thus allowing to study the impact of the fluid molecular complexity

on compressor design and system COP. The VCC components are sized for a worst-case scenario; namely, the helicopter is on the ground on a summer day. The results obtained for the different working fluids are compared in terms of component size and COP, to preliminarily identify the optimal refrigerants.

These system models will be validated by comparison with experimental data generated with the IRIS (Inverse Rankine Integrated System) setup being realized in the laboratory of the Propulsion & Power group of TU Delft. Validated system models will be used in collaboration with commercial partners for the development of new products.

2 VAPOUR COMPRESSION CYCLE SYSTEM

The typical VCC system configuration of a large rotorcraft, utilizing scroll compressors, is shown in Fig. 1. The working fluid commonly adopted is R-134a. Two separate VCC systems cool cabin and cockpit. Each refrigerating loop is equipped with a dedicated condenser with an independent cooling air intake and fan. The cycle configuration is of the intercooler type: a heat exchanger is used to sub-cool the refrigerant entering the expansion valve upstream of the evaporator, thus improving the system performance (Mannini, 1995).

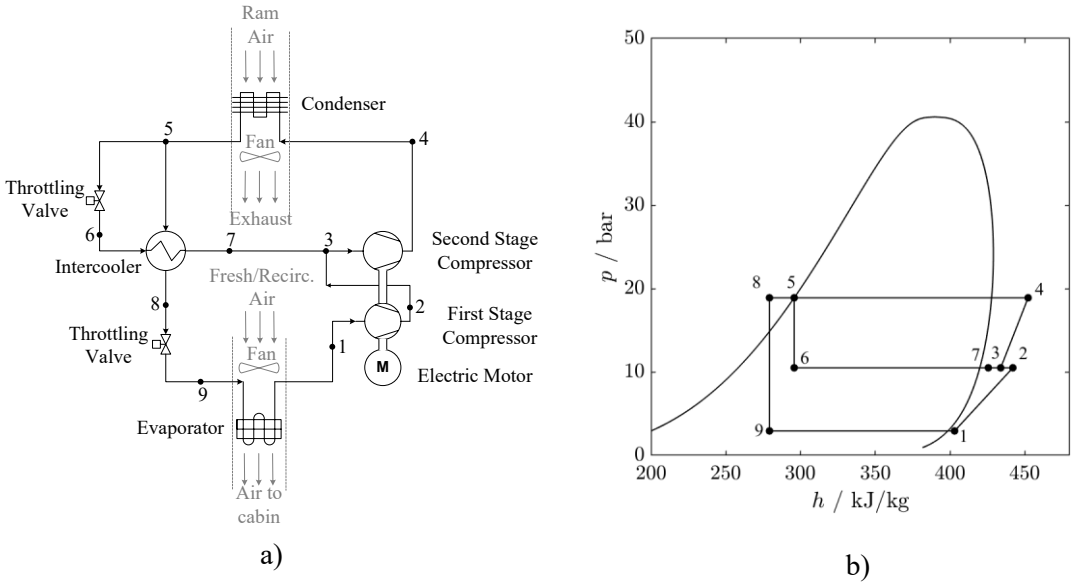

Figure 1: Vapor compression cycle system configuration. a) Simplified process flow diagram; b) Illustration of the processes forming the thermodynamic cycle in the *P-h* diagram of R-134a.

In the baseline configuration, the compressor is of the scroll type, and is mechanically driven by the turboshaft. The condenser is made up of three flat-tube microchannel heat exchangers in parallel on the refrigerant side and in series on the air side. The same type of heat exchanger is adopted for the evaporator. The air entering the evaporator is, to a significant extent, recirculated from the cabin and the cockpit. The ARP-292C (2014) standard prescribes that, for passengers comfort, each occupant should be provided with a fresh air mass flow rate of at least 4.5 g/s in the cabin and 5.6 g/s in the cockpit, while air humidity should not exceed 65%. Cabin air is not pressurized because of the helicopter low flying altitude. Hence, the ratio of recirculated to fresh air is significantly high with respect to a typical aircraft ECS. Both the condenser and the evaporator fans are electrically driven.

The VCC configuration analyzed in this work features an electrically driven centrifugal compressor instead of the traditional scroll machine. Two compression stages are necessary, given the required temperature lift between the condenser and evaporator. The impellers of two compressors are mounted counterposed on the same shaft to minimize the foil bearings' axial thrust.

R-134a is characterized by a high GWP, and thus it will be phased out, also from aerospace applications, in the upcoming years. Therefore, low-GWP working fluids have been considered. In particular, HFOs

are considered as promising working fluids. They exhibit thermodynamic properties similar to those of HFCs, but a significantly lower GWP, since they have a lifetime in the atmosphere of few days (McLinden and Huber, 2020). In addition, they are not flammable and feature low density, which makes them suitable for the design of small capacity centrifugal compressors, like that of the application at hand. Natural refrigerants have also been taken into account due to the high thermodynamic efficiency they generally enable, though their flammability may complicate the system safety certification. Table 1 lists the working fluids considered in the study. The thermodynamic properties are calculated using a well-known software library (Lemmon *et al.,* 2018).

Table 1: List of potential working fluids selected for the application.

Class	ASHRAE name	T_c [K]	p_c [bar]	$\rho_{v,sat_{T=0°C}}\left[\frac{kg}{m^3}\right]$	NBP [K]	σ [K]	$M\left[\frac{g}{mol}\right]$	GWP	ODP	Safety group
HFC	R-134a	374.21	40.49	14.43	247.08	-0.177	109.03	1300	0	A1
	R-32 (Difluoromethane)	351.26	57.82	22.09	221.5	-1.933	52.02	677	0	A2L
	R-152a (Difluoroethane)	386.41	45.17	8.26	249.13	-0.558	66.05	138	0	A2
HFO	R-1234yf	367.85	33.82	17.65	243.67	-0.039	114.04	0	0	A2L
	R-1243zf	376.93	35.18	12.49	247.73	-0.116	96.05	4	0	A2
	R-1234ze(E)	382.51	36.35	11.71	254.18	-0.033	114.04	1	0	A2L
	R-1234ze(Z)	423.27	35.31	3.56	282.88	-0.028	114.04	1	0	A2L
	R-1233zd(E)	439.6	36.24	2.84	291.41	-0.045	130.05	5	0	A1
	R-1224yd(Z)	428.69	33.37	3.76	287.77	0.051	148.49	<1	0	A1
	R-1336mzz(Z)	444.5	29.03	1.82	306.6	0.114	164.06	2	0	A1
Natural refrigerant	R-600a (Isobutane)	407.81	36.29	4.26	261.4	0.131	58.12	4	0	A3
	R-1270 (Propylene)	364.21	45.55	21.40	225.53	-1.284	42.08	2	0	A3
	R-290 (Propane)	369.89	42.51	10.35	231.04	-0.843	44.10	3	0	A3

3 METHODOLOGY

The steady-state model of the VCC system was developed and implemented in the acausal Modelica system modelling language. All the components have been modelled using the lumped parameters approach. The system simulations were used for the preliminary design of both the centrifugal compressor and the heat exchangers for a selected operating point.

3.1 Heat exchangers

As already mentioned, the evaporator and condenser are flat-tube microchannel heat exchangers: the flat tubes feature smaller internal flow passages, i.e. microchannels with circular section. The fins are of the multi-louvered type: several louvers extend along the fin length to augment the heat transfer coefficient on the air side. The heat transfer coefficient can be two to four times higher with respect to plain fins of the same geometry. This kind of CHEXs is also employed in the automotive industry for radiators. The typical compactness factor is around 1100 m^2/m^3 (Zohuri, 2017).

The choice of modelling these devices using a lumped parameters approach stems from the need for a tradeoff between the model complexity and accuracy. The Moving Boundary (MB) method has been preferred to a Finite Volume (FV) discretization method as it allows for a reasonable model accuracy with a relatively low computational cost, as demonstrated by Pangborn *et al.* (2015). The MB method consists in dividing the HEX into a number of control volumes for each refrigerant phase. For instance, the evaporator model accounts for two control volumes. In the first one, the fluid is in a two-phase state (evaporation), while in the second one, it is in a dry vapour state (superheating). The heat transfer coefficient and pressure drop are estimated by implementing different empirical correlations for each control volume, depending on the refrigerant phase. The heat transfer correlations are formulated in terms of Colburn factor *j* or Nusselt number, while the pressure drop calculation is based on the estimate

of the friction factor *f*. Table 2 lists the set of correlations implemented in the HEXs models, for both the refrigerant and air side.

Table 2: List of empirical correlations for the aerothermal design of the HEXs.

Fluid	Property	Reference
Air	Colburn factor	Chang and Wang (1997)
	Friction coefficient	Kim and Bullard (2002)
Refrigerant: single phase flow	Nusselt number	Gnielinski (Kind *et al.*, 2010)
	Friction coefficient	• Hagen-Poiseuille ($\mathrm{Re} < 2.3 \cdot 10^3$) • Blasius ($2.3 \cdot 10^3 < \mathrm{Re} < 2 \cdot 10^4$) • Hermann ($2 \cdot 10^4 < \mathrm{Re} < 2 \cdot 10^6$) • von Kármán ($\mathrm{Re} > 2 \cdot 10^6$) (Kind *et al.*, 2010)
Refrigerant: condensation	Heat transfer coefficient	Shah et al.(1999)
Refrigerant: evaporation	Heat transfer coefficient	Kandlikar (1990)
Refrigerant: two-phase flow	Pressure drop	Friedel (Serth and Lestina, 2014)

In each control volume, the heat transfer rate is estimated based on a correlation between the effectiveness (ε) and the number of thermal units (NTU) of the heat exchanger. The geometrical characteristics of the flat-tube multichannel HEXs are as described by Shah and Sekulic (2003). Finally, the fins dimensions considered for the HEXs are the same indicated in the paper by Kim and Bullard (2002), whose experimental results have been used for the model validation.

It is also worth pointing out that, thanks to the features of the Modelica language, the same heat exchanger model is used for on-design and off-design simulations: in design mode, the operating conditions at the inlet and outlet of the heat exchanger are known, and the model estimate one of the main dimensions (e.g. the flat tube length) of the heat exchanger to meet the required thermal load; in off-design, the geometry is specified, and the heat duty of the heat exchanger is calculated.

3.2 Centrifugal compressor

A mean-line code has been implemented for the preliminary design of the centrifugal compressor. The design variables of the model are: working fluid mass flow rate, total inlet pressure and temperature, flow coefficient Φ, loading coefficient λ, shape factor k, impeller outlet absolute angle α_2, number of blades and diffuser pressure recovery factor C_p. Under the hypothesis of no inlet guide vanes, the flow is assumed to be uniform at the compressor inlet. The design methodology follows the approach proposed by Rusch and Casey (2013). Their work shows that, for a given value of the corrected flow function Φ', see Eq. 1, the optimum inlet metal angle of the impeller is that minimizing the relative inlet Mach number at the impeller shroud, $\mathrm{M}_{w,s1}$. As general design guideline, they also indicate that the value of $\mathrm{M}_{w,s1}$ should not exceed 1.35 to avoid losses due to shocks which may trigger boundary layer separation.

$$\Phi' = \Phi \frac{4\mathrm{M}_{u2}^2}{k\pi} = \frac{\mathrm{M}_{w,s1}^3 \sin^2\beta_{1s} \cos\beta_{1s}}{\left(1+\frac{\gamma-1}{2}\mathrm{M}_{w,s1}^2 \cos^2\beta_{1s}\right)^{\frac{1}{\gamma-1}+\frac{3}{2}}} \tag{1}$$

Given these information, it is possible to solve the static thermodynamic state and the velocity triangle at the inlet of the impeller. The outlet conditions are estimated based on the model proposed by von Backstrom (2006) for centrifugal compressor slip. The internal losses in the impeller (namely blade loading, clearance, mixing and friction) have been estimated using the set of semi-empirical correlations indicated by Oh *et al.* (1997). External losses (recirculation, disc friction and leakage) have been taken into account to determine the total to total efficiency.

Downstream of the impeller, a vaneless diffuser with parallel walls has been considered. The design of the diffuser accounts for the skin friction losses along the channel, according to the model proposed by De Bellis *et al.* (2015). It consists of a non-iterative approach, simplifying the classical set of

conservation equations described by Stanitz (Dubitsky and Japikse, 2008). The main assumptions underpinning their model are that i) the product of the radius and the flow absolute velocity remain constant along the diffuser, and ii) the pressure losses are concentrated at the diffuser outlet. Finally, the compressor model includes a methodology for estimating the axial thrust, based on the set of equations suggested by Tiainen *et al.* (2021).

4 SYSTEM ANALYSIS AND RESULTS

The investigation has been limited to a single design point representative of a critical scenario: the helicopter is on the ground, the environmental air temperature is equal to 40 °C, and the cooling duty is 12.5 kW. Table 3 lists the constraints selected for this application and the values of the design variables of the HEXs and centrifugal compressor. Condensation and evaporation temperatures correspond to the typical operating conditions of a large rotorcraft with 20 passengers and 2 pilots. The condenser dimensions are set equal to those of the current condenser unit of the rotorcraft, while the cooling air mass flow rate is a dependent variable. It is assumed that the air intake size is fixed and the helicopter drag does not increase, while a change in the air pressure drop across the condenser leads to a variation of the cooling air fan power consumption. In the evaporator, the air mass flow rate is prescribed according to the ARP-292C (2014) standard, and the length of the flat tubes is the dependent variable.

Table 3: Operating system conditions and components characteristics.

VCC system for cabin air conditioning					
Refrigerant loop			**Air side**		
Condensation temperature	T_{cond} [°C]	65	Inlet air temperature	$T_{\mathrm{air,env}}$ [°C]	40
Evaporation temperature	T_{evap} [°C]	0	Inlet recirculated air temperature	$T_{\mathrm{air,rec}}$ [°C]	28
Superheating degree	ΔT_{sh} [°C]	5	Fresh air mass flow rate (evaporator)	$\dot{m}_{\mathrm{air,env}}$ [kg/s]	0.1
Temperature difference at pinch point intercooler	ΔT_{pp} [°C]	10	Recirculated air mass flow rate (evaporator)	$\dot{m}_{\mathrm{air,rec}}$ [kg/s]	0.5

Condenser global dimensions		
Width	x [mm]	461
Height	y [mm]	332
Depth	z [mm]	20

Centrifugal compressor design parameters		
Flow coefficient[1]	ϕ [−]	0.1
Shape factor	k [−]	0.9
Isentropic loading coefficient	λ [−]	0.9
Diffuser pressure recovery factor	C_p [−]	0.55
Impeller outlet absolute angle	α_2 [°]	71
Number of blades	−	15

4.1 COP and refrigerant selection

The different working fluids are compared and ranked in terms of system coefficient of performance (COP), see Fig. 2, which is defined as the ratio between the evaporator duty and the compression power:

$$\mathrm{COP} = \frac{\dot{Q}_{\mathrm{evaporation}}}{\dot{W}_{\mathrm{compressor}}} \tag{2}$$

The system COP is strongly influenced by the operating pressure between the two compression stages, hereinafter indicated as intermediate pressure of the system, which is reported on the abscissa of Fig. 2. The highest performances are achieved by the refrigerants belonging to the HFOs group, namely:

[1] The flow coefficient is an independent variable only in the preliminary design of the second stage of the compressor, while it is an output of the preliminary design for the first stage. This is due to the fact in the first stage the rotational speed must be equal to that of the second one.

R-1233zd(E), R-1336mzz(Z), R-1224yd(Z) and R-1234ze(Z). The increase of COP with respect to R-134a ranges from 12% to 15%.

These refrigerants exhibit similar thermodynamic properties, as apparent by examining the shape of the *T-s* diagram in Fig. 3. The slope of the saturation vapour curve of these fluids in the *T-s* graph is slightly positive. This characteristic can be described by the fluid molecular complexity σ, defined as (Angelino and Invernizzi, 1988):

$$\sigma = \frac{T_c^2}{R}\left(\frac{\partial s}{\partial T}\right)_{\text{sat},T_r=0.7} \tag{3}$$

The molecular complexity is directly related to the specific heat capacity c_p of the substance, meaning its ability to store heat: the higher the c_p, the higher the molecular complexity and the more positive the slope of the saturated vapour line. From Fig. 3, it can be observed that the R-134a has a negative slope of the curve, and it is also called wet fluid. R-1336mzz(Z) and R-1234ze(Z) are known as dry fluids due to the positive slope, while R-1233zd(E) and R-1234ze(Z), having nearly a vertical saturation curve, are usually denominated isentropic fluids (Matuszewska, 2020). This chart shows explicitly the advantage of using isentropic and dry fluids in VCC systems, thanks to the lower thermodynamic losses of superheating occurring in the compression process. Though higher molecular complexity generally implies lower latent heat of vaporization, the optimal fluids exhibit lower throttling losses compared to R-134a, which are directly related to the vapour quality at the evaporator inlet. The higher the vapour quality, the higher the thermodynamic losses. However, it is important to remark that fluids with a very high molecular complexity, such as Pentane, can lead to condensation in the compressor, since the compression can end up in a two-phase state, which would damage the blades.

4.2 Centrifugal compressor design

The refrigerants demanding the lower compression power are the four HFOs discussed in the previous section. This power is around 6 kW, with respect to the 6.5 kW required for the R-134a. A design solution is considered feasible only if the axial thrust acting on the bearings is lower than 5 N. This constraint imposes a limitation on the intermediate cycle pressure, as shown in Fig. 4, which reports the trend of COP and axial thrust versus the cycle intermediate pressure for five exemplary refrigerants. The value of intermediate pressure that allows the COP to be maximized is unexpectedly very close to that whereby the net axial thrust becomes equal to zero. This means that the constraint associated with the bearings does not limit the performance of the VCC system. The same conclusion can be drawn for the other fluids considered in the study. The range of intermediate pressure defined by the red dotted lines in Fig. 4 is such that the net axial thrust of the turbomachine remains lower than ±5 N. The results reported in the following correspond to this range of intermediate pressure.

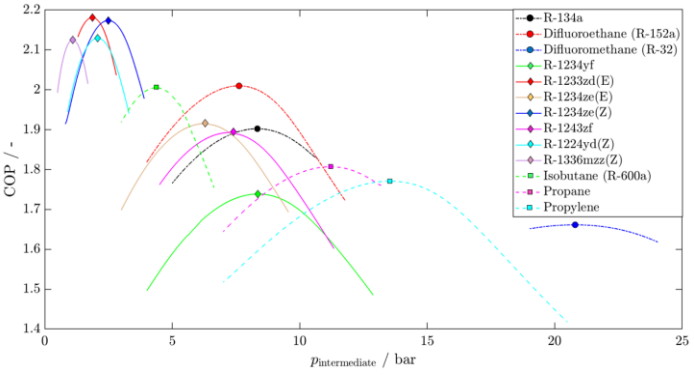

Figure 2: COP versus the system intermediate pressure.

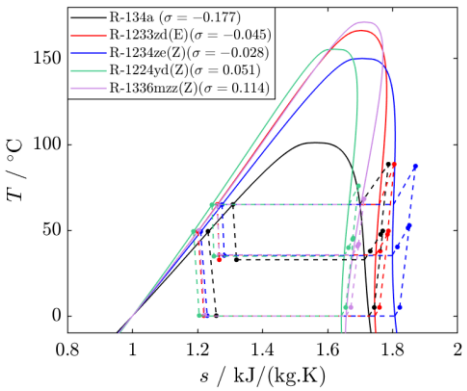

Figure 3: *T-s* thermodynamic chart.

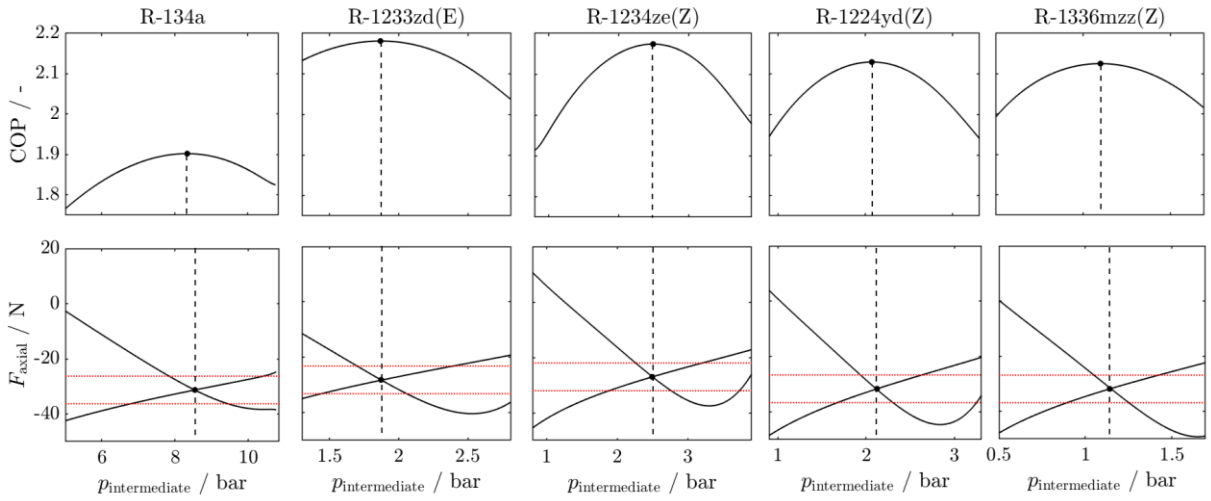

Figure 4: Value of the intermediate pressure setting at zero the net axial thrust of the centrifugal compressor compared to the one maximizing the system COP.

The working fluid characteristics strongly influence the design of the centrifugal compressor. The first stage of the compressor has a compression ratio always higher than that of the second stage. It is also worth noting that the compression ratio of the stages increases considerably with the fluid molecular complexity due to the lower vapour density at the evaporator characteristic of more complex molecules (see Tab. 1). On the other hand, this has a beneficial effect on the volumetric flow rate, as shown in Fig. 5. This represents an advantage for the design of the centrifugal compressors, as a higher volumetric flow rate implies larger flow channels.

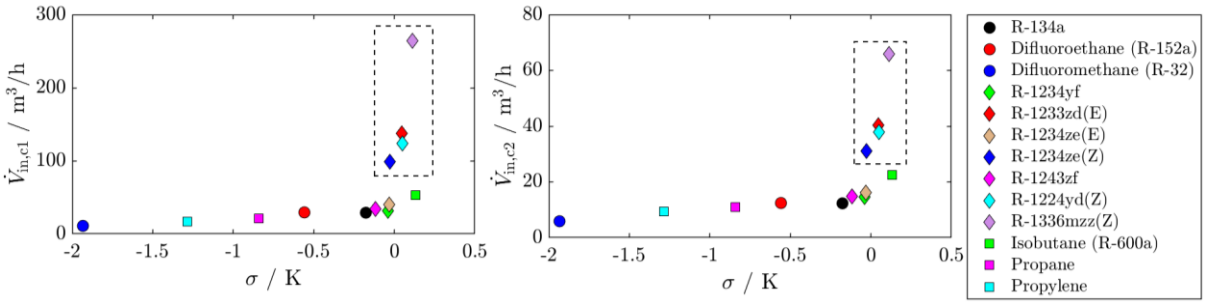

a) b)

Figure 5: Centrifugal compressor volumetric flow rate. a) Inlet volumetric flow rate for the 1st stage; b) Inlet volumetric flow rate for the 2nd stage.

The dimensions of the first compression stage are always larger than those of the second stage. This stems from the higher volumetric flow rate of the first stage and the fact that both stages were designed assuming the same value of flow coefficient, shape factor, and rotational speed. Given the small size of the compressor, it is essential to account in the preliminary design for the limitations that may arise from the manufacturing process. In this regard, a minimum value of 1.3 mm for the outlet channel blade height and a minimum impeller hub radius equal to 2.5 mm have been considered. These requirements are particularly critical for the design of the second compression stage, as they are satisfied only for the HFOs R-1233zd(E), R-1336mzz(Z), R-1224yd(Z) and R-1234ze(Z). However, this comes at the cost of a reduction in the system COP except for the fluid R-1336mzz(Z). As a result of the larger flow passages, the predicted isentropic efficiency of the compressor for these fluids is considerably higher than that estimated for the other compounds. Notably, the fluid enabling the highest isentropic efficiency is R-1336mzz(Z) (~72% in both the stages), but a similar performance is observed for the other HFOs. The feasible design space of the compressor for the different working fluids may benefit from an optimization of the compressor design parameters, see Tab. 3.

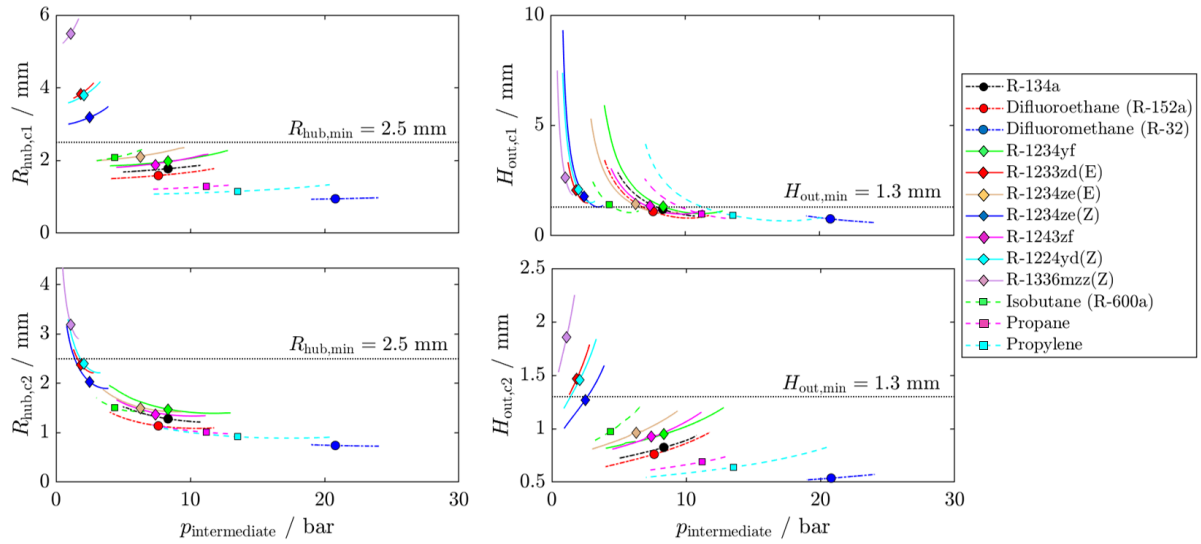

Figure 6: Impeller inlet radius at the hub and outlet radius for the 1st stage (charts at the top) and the 2nd stage (charts at the bottom) of the compressor.

4.3 Heat exchangers design

The heat duty of the condenser is strongly dependent on the COP of the system, reaching a minimum value in correspondence of the intermediate pressure maximizing the system performance. The ram air mass flow rate has the same trend as the condenser duty (Fig. 7). When the system operates with high molecularly complex fluids, the ram air needed for the refrigerant cooling decreases and the minimum values are obtained with the R-1336mzz(Z). Consequently, ram air pressure losses and the required fan power have the same trend.

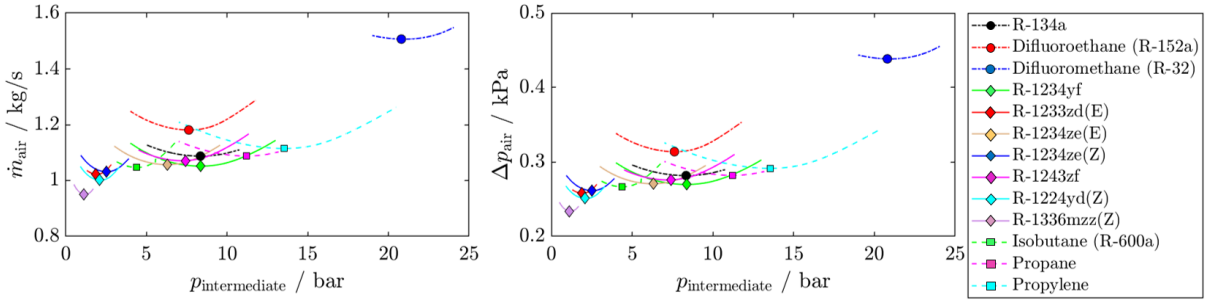

a) b)

Figure 7: Ram air in the condenser. a) Ram air mass flow rate; b) Ram air pressure drop.

Particular attention should be paid to the pressure drop within the HEX. Due to their low density, high molecularly complex refrigerants are characterized by more significant hydraulic losses: the fluid with the highest pressure drop in the condenser is R-1336mzz(Z), as the volumetric flow rate is the highest.

The pressure drop in the working fluid is even more critical in the evaporator, to the point that for the fluids characterized by the highest volumetric flow rates, it has been necessary to increase the number of tubes of the heat exchanger. Notably, the number of tubes was chosen to achieve an average velocity in the evaporator lower than 6 m/s. As a consequence, the weight of the evaporator designed for the molecularly complex refrigerants augments appreciably. Figure 8 shows the results of the estimation of the evaporator dry weight, considering a HEX made of Aluminum, whose density is equal to 2760 kg/m^3. In a system operating with high molecular complexity refrigerants, the global weight of the HEX is almost doubled with respect to the case of HFCs and natural refrigerants, whose weight is ~2.30 kg. In particular, the most critical weight corresponds to 5.8 kg, obtained for a system operating with R-1336mzz(Z), while using the other three HFOs, it reduces to 4.20 kg.

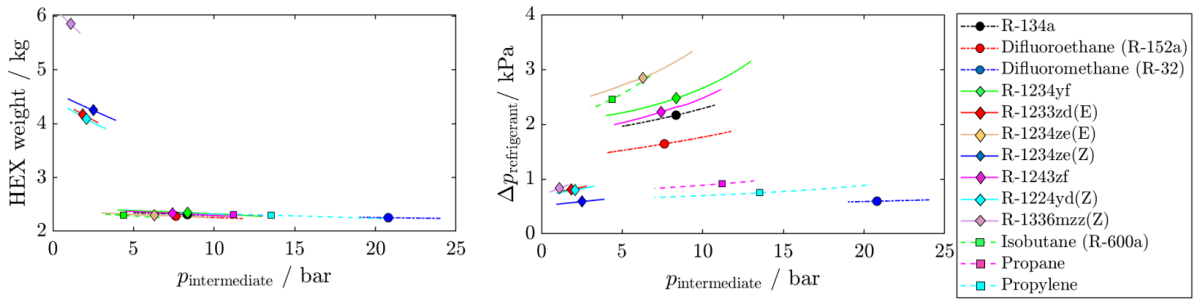

a) b)

Figure 8: Analysis of the evaporator design. a) Dry weight of the HEX; b) Refrigerant pressure drop.

5 CONCLUSIONS

The main conclusions drawn from this study can be summarized as follows:

i) low GWP refrigerants with high molecular complexity represent a valid alternative to R-134a, currently used in VCC systems aboard helicopters. Their high molecular complexity combined with a higher critical temperature allows for lower vapour superheating during the compression and lower vapour qualities at the evaporator inlet. This leads to an increase of the system COP up to 15% if compared to that estimated of R-134a;

ii) the lower density of these HFOs represents an advantage for the design of the centrifugal compressor, since it results in high volumetric flow rates and, hence, in larger flow passages within the compressor as well as lower rotational speeds;

iii) at the same time, the larger volumetric flow rates characteristic of these working fluids demand larger HEXs. If the condenser size cannot be augmented due to restrictions on the dimensions of the cooling air duct aboard the helicopter, it is necessary to increase the cooling air mass flow rate and accept higher pressure drops.

6 NOMENCLATURE

A	HEX total wetted area	(m^2)	$\dot{W}$	mechanical power	(W)
C_p	pressure recovery factor	(-)	**Greek symbols**		
c_p	specific heat capacity	(J/(kg.K))	β_{1s}	inlet relative angle at shroud	(rad)
f	friction factor	(-)	γ	heat capacity ratio	(-)
j	Colburn factor	(-)	λ	loading coefficient	(-)
k	shape factor	(-)	σ	molecular complexity	(-)
M	molecular weight	(g/mol)	Φ	flow coefficient	(-)
$M_{w,s}$	relative Mach number at shroud	(-)	Φ'	modified mass flow function	(-)
M_u	tip Mach number	(-)	ρ	density	(kg/m^3)
p	pressure	(bar)	**Subscript**		
$\dot{Q}$	heat power	(W)	1	inlet section	
R	universal gas constant	(J/(kg.K))	2	outlet section	
s	specific entropy	(J/(kg.K))	c	critical point	
T	temperature	(K)	**Acronyms**		
V	HEX global volume	(m^3)	NBP	Normal Boiling Point	(K)

REFERENCES

Angelino, G. and Invernizzi, C., 1988. General method for the thermodynamic evaluation of heat pump working fluids. *International journal of refrigeration*, *11*(1), pp.16-25.

Chang, Y.J. and Wang, C.C., 1997, A generalized heat transfer correlation for louver fin geometry. *International Journal of heat and mass transfer*, 40(3), pp.533-544.

De Bellis, F., Grimaldi, A., Tommaso Rubino, D., Amirante, R. and Distaso, E., 2015. Accurate Radial Vaneless Diffuser One-Dimensional Model. *Journal of Engineering for Gas Turbines and Power,* 137(8).

Dubitsky, O. and Japikse, D., 2008. Vaneless diffuser advanced model. *Journal of turbomachinery*, 130(1).

Kandlikar, S.G., 1990. A general correlation for saturated two-phase flow boiling heat transfer inside horizontal and vertical tubes. *Journal of Heat Transfer,*112.

Kim, M.H. and Bullard, C.W., 2002, Air-side thermal hydraulic performance of multi-louvered fin aluminum heat exchangers*. International Journal of Refrigeration*, 25(3), pp.390-400.

Kim, M.H. and Bullard, C.W., 2002, Performance evaluation of a window room air conditioner with microchannel condensers. *J. Energy Resour. Technol*., 124(1), pp.47-55.

Kind, M., Martin, H., Stephan, P., Roetzel, W., Spang, B. and Müller-Steinhagen, H., 2010, Heat transfer in pipe flow, *In: VDI Heat Atlas.* Springer.

Kind, M., Martin, H., Stephan, P., Roetzel, W., Spang, B. and Müller-Steinhagen, H., 2010, Pressure Drop in Flow Through Pipes, *In: VDI Heat Atlas.* Springer.

Lemmon, E.W., Bell, I.H., Huber, M.L., McLinden, M.O., 2018, NIST Standard Reference Database 23: Reference Fluid Thermodynamic and Transport Properties-REFPROP, Version 10.0, National Institute of Standards and Technology, Standard Reference Data Program, Gaithersburg

Mannini, A., 1995. The environmental control system for a modern helicopter: a blend. Twenty first European rotorcraft forum.

McLinden, M. O., & Huber, M. L., 2020. (R)Evolution of refrigerants. *Journal of Chemical & Engineering Data*, *65*(9), 4176-4193.

Matuszewska, D., 2020, October. Molecular Complexity of Working Fluids Dedicated to Organic Rankine Cycle (ORC). In *IOP Conference Series: Materials Science and Engineering*, Vol. 946, No. 1, p. 012008, IOP Publishing.

Oh, H.W., Yoon, E.S. and Chung, M.K., 1997, An optimum set of loss models for performance prediction of centrifugal compressors. *Proceedings of the Institution of Mechanical Engineers, Part A: Journal of Power and Energy, 211*(4), pp.331-338.

Pangborn, H., Alleyne, A.G. and Wu, N., 2015, A comparison between finite volume and switched moving boundary approaches for dynamic vapor compression system modeling. International *Journal of Refrigeration*, 53, pp.101-114.

Rusch, D. and Casey, M., 2013, The design space boundaries for high flow capacity centrifugal compressors. *Journal of turbomachinery*, 135(3).

Serth, R.W. and Lestina, T., 2014, Boiling heat transfer, *In: Process heat transfer: Principles, applications and rules of thumb*. Academic press.

SAE AC-9B Subcommittee, 1989. Aircraft Fuel Weight Penalty Due to Air Conditioning (Vol. 1168). Society of Automotive Engineers.

SAE International, 2014, ARP292C: Environmental Control Systems for Helicopters, Aerospace Standard.

Sarlioglu, B., & Morris, C. T., 2015. More electric aircraft: Review, challenges, and opportunities for commercial transport aircraft. *IEEE transactions on Transportation Electrification*, 1(1), 54-64.

Shah, R.K. and Sekulic, D.P., 2003, Heat exchanger surface geometrical characteristics, *In: Fundamentals of heat exchanger design*. John Wiley & Sons.

Tiainen, J., Jaatinen-Värri, A., Grönman, A., Sallinen, P., Honkatukia, J. and Hartikainen, T., 2021. Validation of the Axial Thrust Estimation Method for Radial Turbomachines. *International Journal of Rotating Machinery*, 2021.

von Backstrom, T. W. , "A Unified Correlation for Slip Factor in Centrifugal Impellers", *Journal of Turbomachinery*, 2006.

Zohuri, B., 2017, Compact heat exchangers design for the process industry, *In:Compact heat exchangers*. Springer.